JOURNAL OF SOLID STATE CHEMISTRY 49, 166–179 (1983)

Growth and Characterization of n-WS_2 and Niobium-Doped p-WS_2 Single Crystals

J. BAGLIO,[1] E. KAMIENIECKI, N. DECOLA, AND C. STRUCK

GTE Laboratories, Inc., Sylvan Road, Waltham, Massachusetts 02254

AND J. MARZIK, K. DWIGHT, AND A. WOLD

Department of Chemistry, Brown University, Providence, Rhode Island 02912

Received February 9, 1983, and in revised form April 18, 1983

Single crystals of n- and p-WS_2 were obtained by chemical vapor transport using chlorine and bromine as transporting agents. The best niobium-doped WS_2 crystals were obtained when the concentration of the charge (formulated $(1 - x)WS_2 \cdot (x)NbS_2$) was ≈37 mg charge/ml of tube, and $x = 0.01$ to 0.03. A thermodynamic analysis of the crystal growth process is consistent with the observed doping concentration and other properties of the crystals obtained by this process. The crystals grown are characterized by electrical transport and surface photovoltage measured capacitance techniques.

Introduction

The most serious problem associated with the use of semiconductor electrodes in photoelectrochemical devices is their susceptibility to photodecomposition. The transition metal dichalcogenides are attractive semiconductor materials for use in photoelectrochemical energy conversion processes because they are not as susceptible to photocorrosion as are many other materials whose band gaps are in the region of maximal solar conversion efficiencies.

Tributsch (*1*) concluded in 1977 that these materials should be resistant to photocorrosion because their highest valence band and lowest conduction band are formed by nonbonding *d*-electronic states of the transition metal atoms. He suggested that electronic excitation would not affect the bond between the metal and the chalcogen atoms leading to kinetic stability of these materials.

These layered compounds indeed show unusual resistance against photocorrosion under some circumstances. However, their corrosion sensitivity increases if the surface contains structural defects such as steps. It also has been pointed out that the corrosion resistance of chalcogenide materials is due to the fact that the electronic states of the highest valence band and lowest conduction band are largely shielded from interaction with possible reactants in solution by the compact layers of the chalcogen atoms (*2*). At defects in the surface and at steps, however, this shielding is lost and the transition metal as well as chalcogen atoms can easily interact with the components from the electrolyte. There are two

[1] To whom all correspondence should be addressed.

0022-4596/83 $3.00

Copyright © 1983 by Academic Press, Inc.
All rights of reproduction in any form reserved.

important consequences of these defects. First, corrosion begins at such sites and, second, these unsaturated bonds result in electronic states which appear to be located within the band gap and act as recombination sites. The presence of surface states together with the anisotropic mobilities of these compounds are normally used to explain the poor power characteristics and conversion efficiencies of crystals containing imperfect surfaces (*3*).

While there have appeared several publications on the growth of $MoSe_2$, MoS_2, WSe_2, and WS_2 compounds, a review of the published work reveals that there are critical problems associated with the growth of single crystals of MY_2 compounds. While crystals have been grown by chemical vapor transport using chlorine, bromine, and iodine as transport agents, difficulties were encountered in reproducibly preparing good quality crystals of a single crystallographic modification and controlled doping concentrations (*4–10*). While previous studies (*10, 11*) have discussed the electrochemical properties of n-WS_2 and have presented some of the procedures that were used in growing these crystals, nothing has been published on the growth of p-WS_2 or p-MoS_2. In this paper, the techniques used to grow n-WS_2 will be described. The modifications that are necessary to grow p-WS_2 and p-MoS_2 will be presented. A correlation of growth temperatures, niobium doping concentrations, and predictions from thermodynamic analysis with analytical electrical transport and electrochemical data is presented to help create a better understanding of the growth process.

Experimental Procedures

Crystal growth. The single crystals of n- and p-WS_2 were grown in fused silica ampoules by halogen vapor transport. The silica tube (1.1 cm diam × 25 cm length) was normally loaded with 37 mg of polycrystalline charge/ml of tube formulated as $(1 - x)WS_2 \cdot (x)NbS_2$ with $x = 0$ for n-WS_2 and $x = 0.005$ to 0.05 for p-WS_2. The polycrystalline charge was previously prepared by heating tungsten powder (Spex Industries, metal impurities <10 ppm), sulfur (Gallard Schlesinger 99.999%), and niobium (Atomergic Chemetals 99.8%) in an evacuated and sealed silica tube, to 1000°C. The procedures that were used to grow n- and p-MoS_2 are the same as those used for WS_2 with the molar concentrations of the charges being identical. Molybdenum powder (Atomergic Chemetals 99.99% excluding W) was used for the synthesis of MoS_2.

The crystal growth of n-WS_2 (MoS_2) was accomplished by vapor transport with either Br_2 with concentration 5 mg/ml of tube or Cl_2 with concentration of 3 or 0.3 mg/ml of tube. The growth of p-WS_2 (MoS_2) was best accomplished by chlorine transport of a niobium-doped charge (concentration range $x = 0.01$ to 0.03) with the chlorine concentration at 3 mg Cl_2/ml of tube. In several cases, WO_2 (Materials Research Corporation 99%) was used as an oxygen source (see Single Crystal Growth below). In addition, a stoichiometric amount of sulfur to form WS_2 was added to the reaction tubes. The typical temperature profile of the three-zone furnace that was used during the growth of both n- and p-WS_2 is shown in Fig. 1. The procedures for evacuating and filling the silica tubes, as well as those associated with pre-growth temperature profiling, have been described previously (*11*). In all cases, the growth process was terminated before all of the charge was transported.

Thermodynamic analysis. A thermodynamic analysis of the growth process involved the use of a NASA chemical equilibrium computer program (*12*). This program considers all reactants and possible products contained in its data set, and minimizes the free energy under mass balance constraints to obtain equilibrium composi-

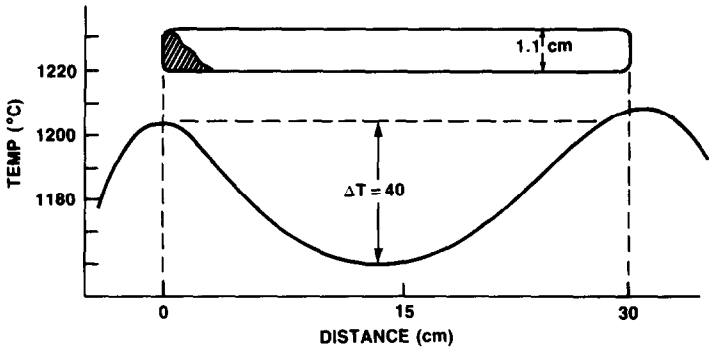

FIG. 1. Temperature profile of three-zone furnace.

tions. The thermodynamic data supplied with the original program has been updated. References include JANAF thermochemical tables (*13*, *14*) and others cited (*15–18*).

In several instances, only the room temperature values of the thermodynamic quantities are available. In order to obtain values of ΔH_T, S_T, and $C_{p\,T}$, up to $\simeq$1500 K, it was necessary to estimate ΔC_p versus T. The extrapolation of C_p from room temperature data to those at higher temperatures was accomplished by assuming that the change in heat capacity with temperature paralleled that of similar compounds. Because of the uncertainties associated with the data, the equilibrium constants calculated from these data sets may be in error by an order of magnitude or more. The results of the thermodynamic analysis are not given quantitative significance, but are used as a guide to understanding the growth process. The substances considered in the equilibrium calculations include the carbides, elements, halides (bromides and chlorides), oxides, oxyhalides, oxyhydroxides, and the sulfides. There are, however, no data available for niobium oxybromides or oxyhydroxides. Hence, calculations based on the combined metal, oxide, halide, and sulfide systems were limited to chlorine as the halogen when niobium was included as one of the metallic components.

Capacitance voltage and electrochemical techniques. The capacitance as a function of the electrode potential (Mott-Schottky plot) was measured using the surface photovoltage measured capacitance (SPMC) technique. This method permits the space-charge capacitance to be determined from the changes of the surface potential barrier, which is induced by chopped light of photon energy exceeding the bandgap of the semiconductor. At low intensity, the measured SPMC signal is proportional to the reciprocal of the semiconductor surface space-charge capacitance C_{sc}. The proportionality factor is entirely determined by the modulation frequency of the light, the incident photon flux, and the reflection coefficient of the semiconductor (*11*).

In the depletion region, when C_{sc}^{-2} is proportional to the electrode potential, the slope of the Mott-Schottky plot gives the doping concentration in the space-charge region. In estimating the doping concentration of WS_2, a value of 10 for the dielectric constant has been used. The techniques used in photoelectrochemical investigations of these materials include cyclic voltammetry and steady-state current voltage measurements in nonaqueous and aqueous electrolytes containing redox couples which span the energy positions of the band edges (*11*). Electrical contacts

were made between the crystal and copper wire using Ga–In alloy plus silver epoxy.

Hall effect. The Hall effect was measured by the van der Pauw method, using a Varian 4-in. electromagnet (Model V-4004) to produce a magnetic field of 6.7 kOe. A constant current of 0.1 mA from a PAR reference source (Model TC-100.2 AR) was passed through the sample, and the resulting voltages were detected with a Hewlett–Packard autoranging digital voltmeter (Model 3450A). Electrical contacts were made with colloidal graphite (Electrodag, Acheson Colloids Co.).

Results and Discussion

Nature of Polycrystalline Charge

X-Ray diffraction analysis of polycrystalline samples, formulated as $(1 - x)WS_2 \cdot (x)NbS_2$, prior to their use in the halogen transport process, indicated that, within the range of interest $x = 0$ to $x = 0.3$, these disulfides form a series of solid solutions. The crystal structure of these samples was found to be hexagonal (2H), while polycrystalline niobium sulfide prepared under similar conditions was found to form with the rhombohedral (3R) structure (*19*). The diffraction patterns from the solid solutions broadened with increasing concentration of niobium. This broadening was not limited to those reflections ($H - K = 3N \pm 1$; $N =$ 0 or integer) normally attributed to stacking faults in these materials (*20*). The broadening was, therefore, interpreted as indicating some inhomogeneous distribution of niobium within WS_2.

X-Ray diffraction and compositional (emission spectrographic and spark source mass spectrographic) analyses of the polycrystalline materials that remained in the charge zone, subsequent to being subjected to the (Cl_2) vapor transport growth process, demonstrated sharp diffraction peaks and at least an order of magnitude decrease in the niobium concentration. Results indicated that niobium is preferentially being depleted from the polycrystalline charge during the growth process. In the thermodynamic analysis described below, it will be shown that niobium remains in the vapor phase. X-Ray diffraction and compositional analysis further demonstrated that SiO_2 (from the silica transport tube) was being transported to the higher temperature zones.

Single Crystal Growth

Aggarwal *et al.* (*8*) have reported that single crystals of WS_2 can be grown by a sublimation method without the addition of a transporting agent. According to these authors, polycrystalline WS_2 powder was heated at temperatures between 1020 and 1050°C with a gradient of approximately 20°C across the 21-cm tube length. Their crystals were reported to be in the form of large ($10 \times 4 \times 0.2$ mm) platelets and were distributed throughout the ampoule. Attempts to use this technique to grow crystals of sufficient quality to be used as electrodes in photoelectrochemical cells were unsuccessful. The crystals were small and gave poor photoelectrochemical response with large dark currents. The crystals were subsequently grown by chlorine and bromine transport techniques.

As shown in Table I, the quality of n-type single crystals was strongly affected by the temperature of the growth process and not strongly dependent on either the nature or the concentration of the transporting agents. This was not found to be true for the growth of p-WS_2. In this case, it was found that the nature and concentration of the transporting agent was also critical for the growth of good quality single crystals. Earlier attempts to grow single crystals of p-WS_2 using iodine as the transporting agent with $x = 0$, as has been accomplished with $MoSe_2$ (*4*), were unsuccessful. The best p-type crystals were subsequently obtained by chlorine vapor transport of the (1

TABLE I
CRYSTAL GROWTH CONDITIONS

Charge (g)	Chlorine concentration (mg/ml of tube)	Temperature profile (°C)			Time (hr)	Dimensions (cm)	Comments (quality)[a]
		Charge	Growth	End			
WS_2(1.1)	3.0	1200	1140	1210	100	(1.0 × 1.0 × 0.01)	Good
WS_2(1.1)	0.3	1200	1140	1210	160	(0.5 × 0.6 × 0.01)	Good
WS_2(1.1)	3.0	1070	1030	1080	200	(0.2 × 0.2 × 0.01)	Poor
WS_2(1.1)	0.3	1070	1030	1080	250	(0.2 × 0.2 × 0.01)	Poor
W+S(1.84, 0.64)	5.5 (Br_2)	1175	1125	1175	120	(0.4 × 0.5 × 0.01)	Good

Note. Tube fused silica (30 cm long, 1.1 cm O.D.) prepumped to 1×10^{-5} atm.

[a] Good—equivalent to low dark currents and single crystal diffraction patterns. Poor—equivalent to large dark currents and polycrystalline diffraction patterns.

$-x)WS_2 \cdot (x)NbS_2$ materials. Niobium was not detected in the single crystals that were obtained under the preferred conditions (i.e., with 37 mg $(1-x)WS_2 \cdot (x)NbS_2$/ml of tube, with $x = 0.005$ to 0.05; and 3 mg Cl_2/ml of tube). Since tungsten lines strongly interfere with the mass spectrographic analysis for niobium, the result is interpreted to mean that the niobium concentration in peeled samples (to remove surface impurities) was less than 40 ppm. In order to assure ourselves that niobium could indeed be incorporated into the crystals as a dopant, single crystals of p-MoS_2 were grown under the identical conditions as the tungsten analog. Molybdenum lines do not interfere with the determination of niobium. With composition of the $(1-x)MoS_2 \cdot (x)NbS_2$ charge at $x = 0.02$, the mass spectrographic analysis indicated that the concentration of niobium in the peeled sample was $\simeq$5 ppm. Moreover, it was found that either an addition of large amounts of niobium (i.e., $x > 0.10$) to the 37 mg of charge/ml of tube, or an increase in the concentration of the charge in the tube to 150 mg/ml of tube while maintaining the mole fraction of NbS_2 constant (i.e., $x = 0.03$), caused the transport of WS_2 to stop.

In order to optimize the growth process and help explain some of these observations, a thermodynamic analysis was undertaken. A major uncertainty associated with this analysis is the unknown influence of the growth chamber (silica tube) on the nature and concentration of the vapor phase species. In view of the analytical data indicating that SiO_2 transports under the conditions used to grow n- and p-WS_2, the silica tube was considered an active species in the thermodynamic analysis. Figure 2 shows the partial pressures of all components (above 10^{-4} atm) in the vapor phase. The solid phases (which are not shown) were obtained from this analysis, and consist of $WS_{2(s)}$ and $SiO_{2(s)}$. All niobium is calculated to be in the vapor phase. The results shown in Fig. 2 demonstrate that the major components of the vapor phase consist of S_2, WO_2Cl_2, $SiCl_4$, and $NbOCl_3$, and the minor components include WCl_4, SO_2, Cl_2, and Cl, as well as $NbCl_5$. The important conclusions drawn from this analysis are: all the niobium is in the vapor phase, with the only solid phases being SiO_2 and WS_2, with SiO_2 transported in the opposite direction from WS_2. Increasing the concentration of niobium in the charge, or increasing the amount of charge in the tube, increases the relative concentration of $NbOCl_3$ and $NbCl_5$ in the vapor phase compared to WO_2Cl_2 and WCl_4 (see Fig. 3). In Fig. 3, the

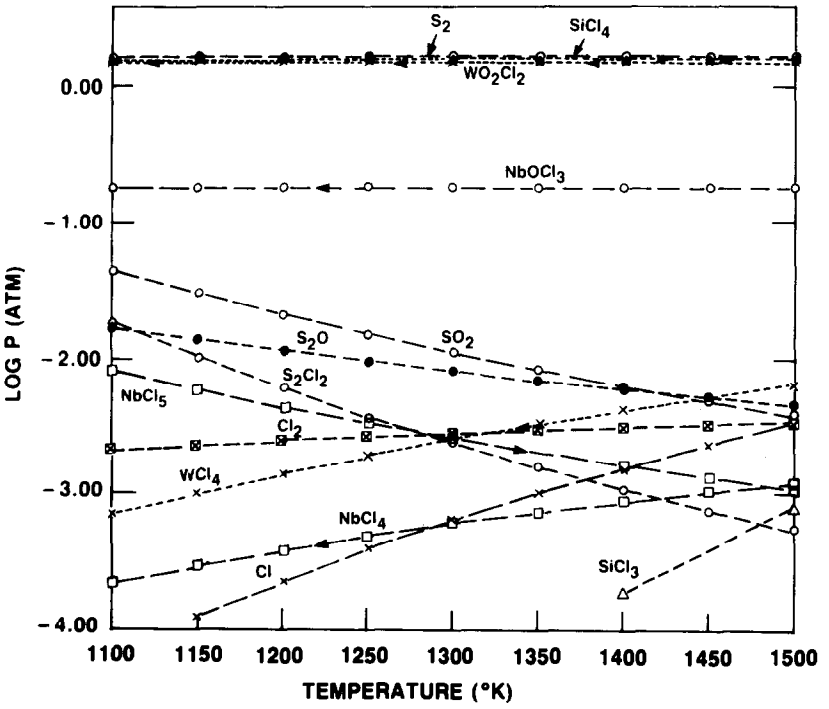

FIG. 2. Thermodynamic analysis of the system containing 4.455 mmole $WS_{2(s)}$, 0.0456 mmole $NbS_{2(s)}$, 1.18 mmole Cl_2, and 3 mmole SiO_2. Total pressure 5 atm.

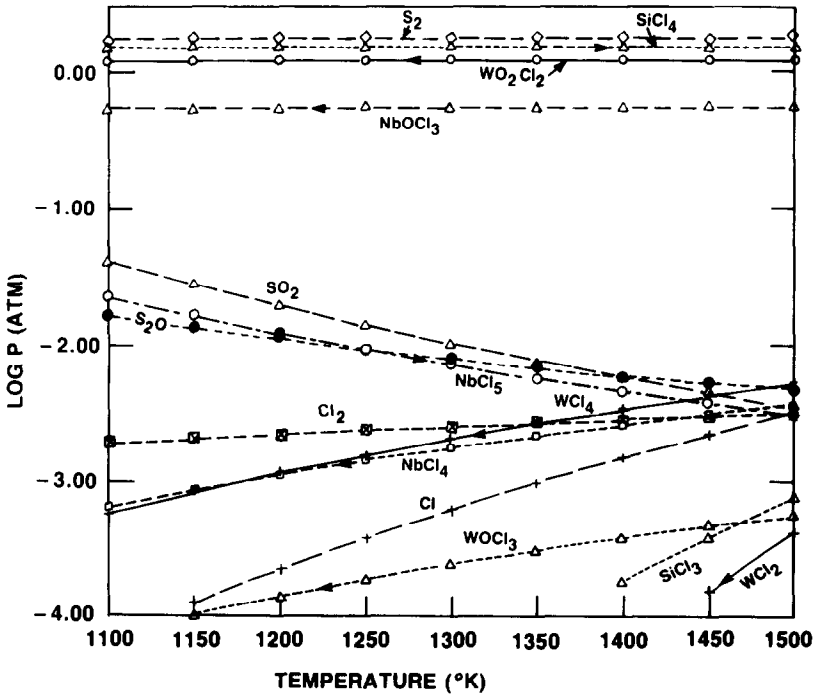

FIG. 3. Thermodynamic analysis of the system containing 0.13 mmole $NbS_{2(s)}$. Other conditions as Fig. 2.

solid phases consist of only $WS_{2(s)}$ and $SiO_{2(s)}$ with all of the niobium calculated to be in the vapor phase. Finally, when the concentration of niobium in the tube is increased to a point where solid NbS_2 is calculated to be transported (as $NbOCl_3$ and $NbCl_5$), the concentration of $WO_2Cl_{2(g)}$ and $WCl_{4(g)}$ goes to zero. Hence, at this point, the transport of WS_2 ceases (see Fig. 4). In Fig. 4, the solid phases (which are not shown) consist of $WS_{2(s)}$, $SiO_{2(s)}$ as well as NbS_2 below 1400 K. Above 1400 K, all niobium remains in the vapor phase. Consequently, under the conditions used to grow good single crystals of p-WS_2, the niobium concentration in the crystal would be limited to that of a minor impurity even though relatively large amounts are added to the charge.

In order to show that these conclusions are not strongly influenced by the uncontrolled amount of silica that is transported, two further experiments were performed. First, a thermodynamic analysis was carried out assuming either chlorine or bromine as the transporting agent and silica as an inert container. The results from this analysis demonstrated the same phenomena; i.e., under the preferred conditions for growth of WS_2, all the niobium remains in the vapor phase and, when NbS_2 begins to be transported, the growth rate of WS_2 goes to zero. The major vapor species in these cases are S_2, WCl_4, and $NbCl_5$, or WBr_5 and $NbBr_5$ when chlorine or bromine is used as the transporting agent, respectively. The second experiment was the addition of oxygen to the growth tube by means of $WO_2 + 2S$. The number of moles of oxygen added by this method was

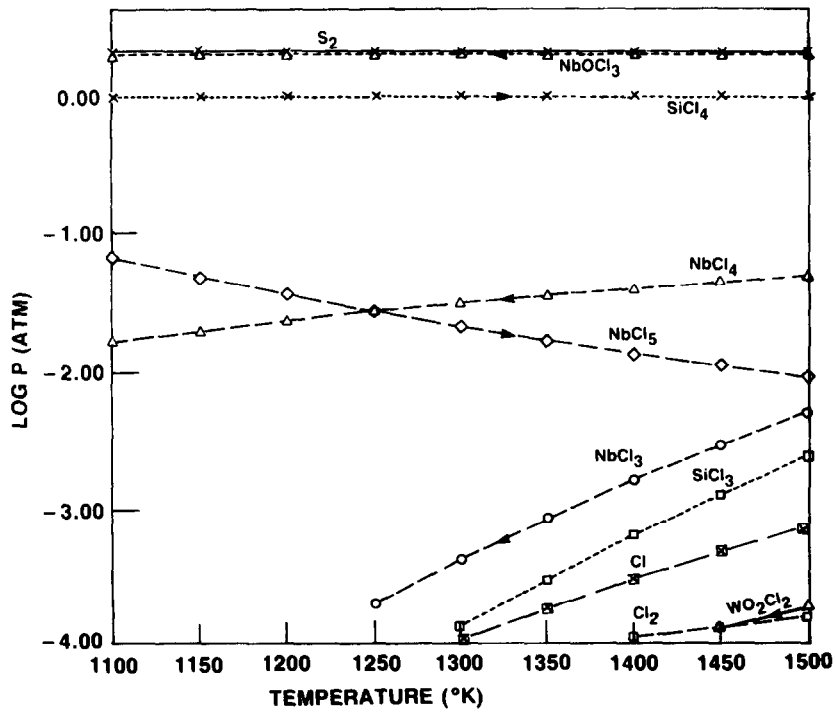

FIG. 4. Thermodynamic analysis of system containing 13.08 mmole WS_2, 0.5 mmole of NbS_2, 1.18 mmole Cl_2, and 3 mmole SiO_2. Total pressure 5 atm. Pressure of S_2Cl_2 and S_2O (log $P \sim -3.5$) not shown.

slightly less than that of chlorine, in order to keep the pressure in the tube at less than 10 atm (at 1200°C). Under these conditions, the major components of the vapor phase are calculated to be S_2, WO_2Cl_2, and $NbOCl_3$, whose concentrations are almost independent of the formation of $SiCl_4$ within the silica tubes. It was found that good quality single crystals of both n- and p-WS_2 were formed by this process and that the change in carrier type was accomplished by the addition of niobium to the charge.

The thermodynamic analysis was also used to investigate the sublimation process described by Aggarwal *et al.* (*8*). The first assumption was that the transition metal sulfides would transport via the reaction $MS_{2(s)} = MS_{(g)} + \frac{1}{2}S_{2(g)}$. Niobium sulfide was used as the model compound for this study, since there are thermodynamic data available for $NbS_{2(s)}$, $NbS_{(s)}$, and $NbS_{(g)}$, while none are available for the $WS_{(g)}$ counterpart. The results shown in Table II demonstrate that even at 1450 K, where niobium disulfide decomposes to $NbS_{(s)}$ and $S_{(g)}$, negligible amounts of $NbS_{(g)}$ exist in the vapor phase. Consequently, the transport of NbS_2 via $NbS_{(g)}$ should be extremely slow. Schafer and Schulte (*16*) previously reported that the chemical transport of MoS_2 and WS_2 in the presence of iodine proceeds via the oxyiodides MoO_2I_2 and WO_2I_2. The oxygen is being obtained from H_2O which is liberated from the walls of the quartz tubes. In view of this, a thermodynamic analysis was also performed on the system WS_2, NbS_2 (1 atomic%), H_2O. The results (shown in Table III) demonstrate that, even when a relatively large concentration of H_2O is assumed to be present in the tube, transport by $WO_2(OH)_2$ type species is negligible. Consequently, transport of WS_2 by sublimation is not verified by these analyses.

TABLE II

THERMODYNAMIC CALCULATION FOR NbS_2, ARGON SYSTEM

Chemical formula	Input (mole fraction)	Output (mole fraction)[a] 1450 K	1400 K
Ar	2.2×10^{-5}	1.5×10^{-5}	2.2×10^{-5}
$NbS_{2(s)}$	0.99998	0.0	0.99998
$NbS_{(s)}$	—	6.7×10^{-1}	7.9×10^{-7}
$NbS_{(g)}$	—	1.0×10^{-10}	1.1×10^{-15}
$S_{(g)}$	—	7.4×10^{-4}	3.5×10^{-9}
$S_{2(g)}$	—	3.3×10^{-1}	3.9×10^{-7}

[a] Total pressure = 1×10^{-4} atm.

TABLE III

THERMODYNAMIC CALCULATION FOR WS_2, NbS_2, H_2O SYSTEM

Chemical formula	Input (Mole fraction)	Output (mole fraction)[a] 1450 K	1400 K	1350 K
$WS_{2(s)}$	0.9648	0.9679	0.9682	0.9685
$NbS_{2(s)}$	0.00966	8.0×10^{-4}	7.8×10^{-4}	7.5×10^{-4}
H_2O	0.02556	3.4×10^{-3}	3.4×10^{-3}	3.3×10^{-3}
H_2	—	6.9×10^{-3}	6.3×10^{-3}	5.8×10^{-3}
H_2S	—	1.5×10^{-2}	1.6×10^{-2}	1.7×10^{-2}
S_2	—	1.2×10^{-3}	9.0×10^{-4}	6.4×10^{-4}
$WO_2(OH)_{2(g)}$	—	5.6×10^{-11}	2.4×10^{-11}	9.3×10^{-12}
$Nb_2O_{5(g)}$	—	4.4×10^{-3}	4.5×10^{-3}	4.5×10^{-3}

[a] Total pressure = 5 atm.

Characterization of Single Crystals

A strong correlation was found to exist among estimates of crystal perfection, electrochemical performance, and the temperature of the growth zone (with the temperature gradient maintained at 50°C). The best crystals were obtained when this temperature was at ≈1150°C. Under these conditions, the crystals usually grew in the form of flat plates whose dimensions were up to 1 × 1 × 0.02 cm thick. The larger dimensions are controlled by the diameter of the silica tube (1.1 cm). X-Ray diffraction data taken from these crystals (as exemplified in Fig. 5) indicate that they are single crystals of the hexagonal (2H) modification. Optical and electron microscopic examinations of these crystals indicated that they contained a low density of steps, and electrochemical

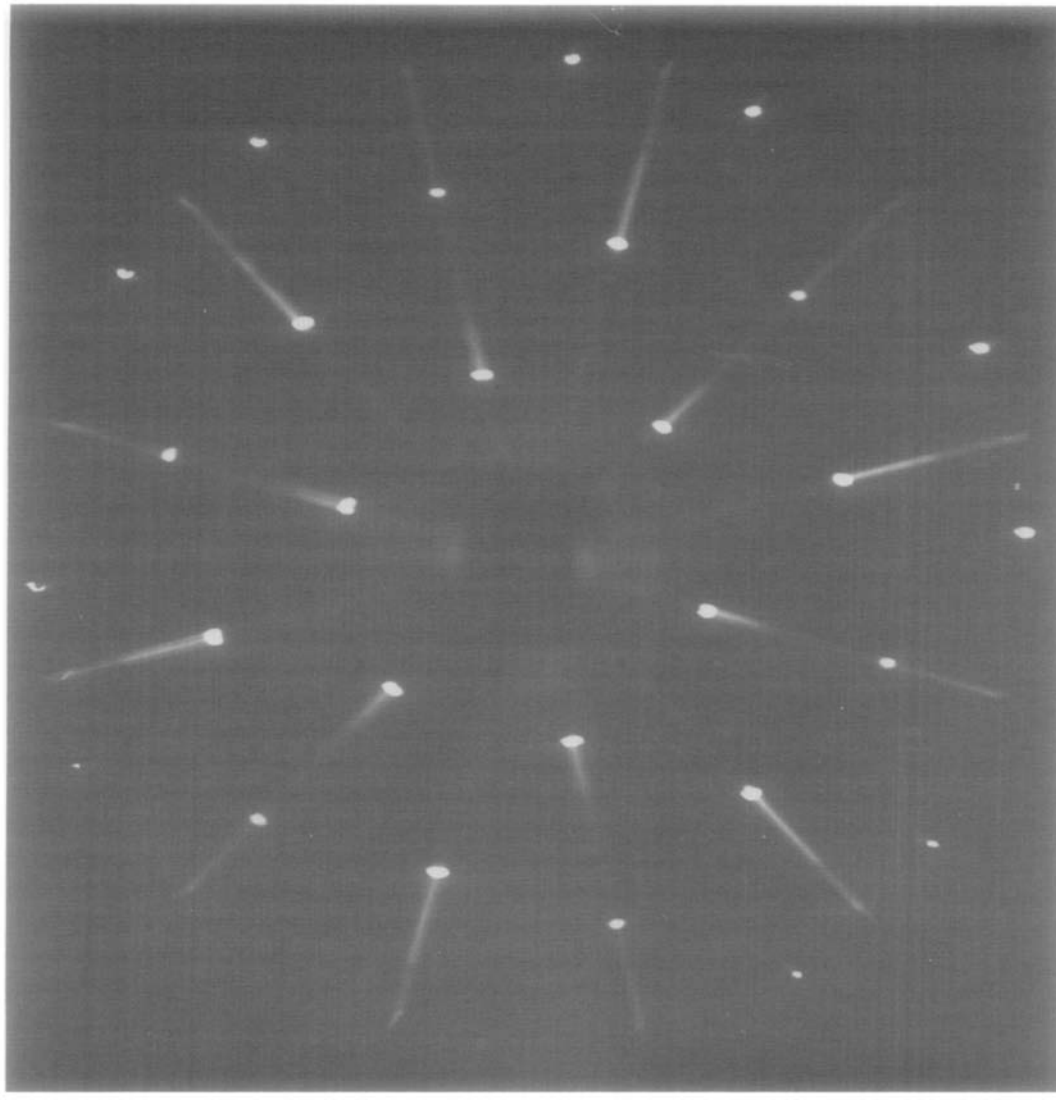

FIG. 5. Zero-layer precession photograph of WS_2.

analysis showed that peeled samples revealed negligible dark currents. From Auger analysis of the surface of the as-grown crystals, the silicon concentration was estimated to be as large as 20 atomic%, and the oxygen concentration up to 40 atomic%. Nondetectable amounts of silicon and O_2 in the sample were obtained by either peeling $\simeq$20 μm off the sample with adhesive tape (which exposes a fresh surface) prior to analysis, or by sputter etching $\simeq$1500 Å from the sample. The emission spectrographic analysis of peeled samples (shown in Table IV) indicates the level of impurities that are normally observed in these semiconductors.

Crystals prepared at lower temperatures (<1100°C) grew in the form of rose petals. The X-ray diffraction patterns of these crystals indicated polycrystalline regions

TABLE IV
IMPURITY LEVELS IN MoS_2 AND WS_2 SINGLE CRYSTALS

Element	ppm wt			
	A[a]	B[a]	C[b]	D[b]
Na	5.8	9.2	2.4	5.4
Al	0.36	0.20	0.2	0.4
Si[c]	3.5	1.1	1.4	2.2
Cl[c]	77	33	48	76
K	0.91	90	0.7	1.3
Ca	1.9	1.8	1.2	2.0
Cr	3.4	0.19	0.4	0.5
Mn	0.21	ND	ND	ND
Fe	18	1.5	0.8	2.0
Co	ND	6.2	ND	ND
Se	1.7	ND	ND	ND
Nb	4.1	1.6	ND	ND
Cd	1.9	0.99	ND	ND
In	0.12	0.12	ND	ND
Ba	0.06	ND	ND	ND
W(Mo)	24	64	(0.5)	(0.5)
Pb	ND	ND	ND	ND
Bi	ND	ND	ND	ND

[a] Peeled crystals of MoS_2.
[b] Peeled crystals of WS_2.
[c] Less than.

and/or twinning. Optical microscopic observations of these crystals revealed the presence of many steps, while electrochemical results demonstrated poor photoelectrochemical behavior and large dark currents.

Electrical Transport Properties

As shown in Fig. 6, the net doping and carrier concentration increases with increasing the number of moles of niobium in the tube. The net carrier concentrations were obtained from Hall-effect measurements, and the net doping concentrations from surface photovoltage measured capacitance data (*11, 12*). Table V shows the effect of niobium on room temperature conductivity and mobility. In most cases, the mobility ($\perp c$-axis) was higher for p-WS_2 than n-WS_2 which indicates that the mobility of holes is somewhat greater than electrons in these materials. At high concentrations of niobium ($x = 0.5$), the mobility decreases. This is attributed to the large concentration of defects (steps) which were found in crystals that were prepared from a charge containing such high molar concentrations of niobium.

It was also found that crystals grown from $(1 - x)WS_2 \cdot (x)NbS_2$ with $x = 0$ and $x = 0.01$ to 0.03 are uniform, with low density of steps. Crystals with $x \simeq 0.004$ had nonuniform doping concentrations, as demonstrated by the presence of both p and n domains.

Figure 7 compares the net hole concentration with net doping concentration in p-WS_2. For doping concentrations above $\simeq 10^{17}$ (atomic% Nb ≥ 1 in Fig. 6), the slope of the straight line indicated that the hole concentration is proportional to the square root of the net doping concentration. This result is consistent with the behavior expected for noncompensated materials (*22*).

The temperature dependence of mobility

TABLE V
CHARACTERIZATION OF WS_2:Nb[a] BY HALL AND CONDUCTIVITY MEASUREMENTS

Nominal concentration of Nb (atomic%)	Conductivity type	Conductivity (Ω^{-1} cm^{-1})	Mobility (cm^2/Vs)
0	n	0.03	135
0[b]	n	0.03	150
0[c]	n	0.04	103
0.4	p[d]	0.1	250
0.5	p	0.9	270
1.0	p	2.2	290
2.0	p	4.8	270
4.5	p	6.7	70

[a] Normally grown using 3.0 mg Cl_2/ml of tube as transporting agent, temperature 1200 to 1150°C.
[b] Transporting agent Cl_2 (0.3 mg Cl_2/ml of tube).
[c] Transporting agent Br_2 (6.7 mg Br_2/ml of tube).
[d] Nonuniform n + p domains.

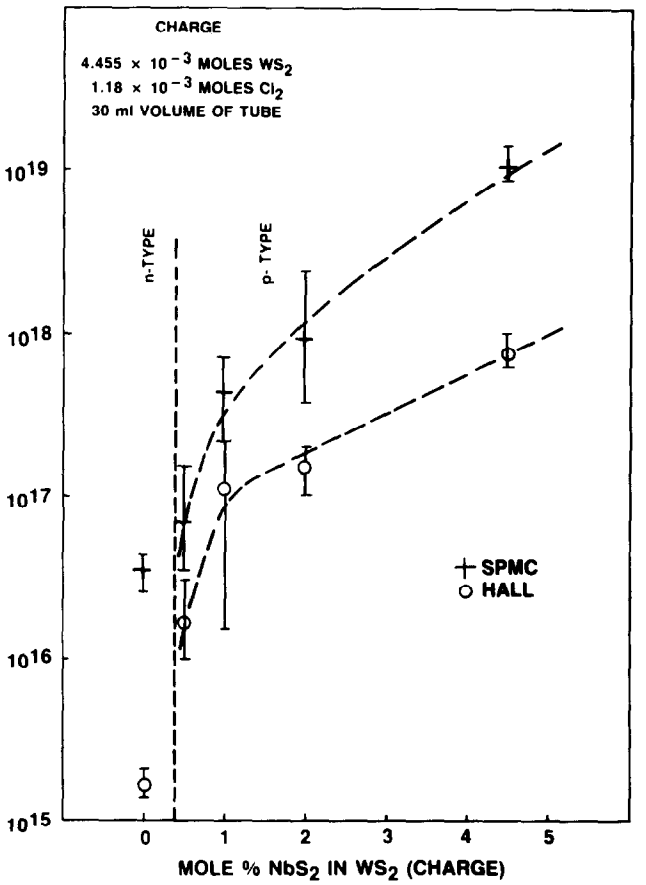

FIG. 6. Net doping and net carrier concentration versus niobium concentration in the charge.

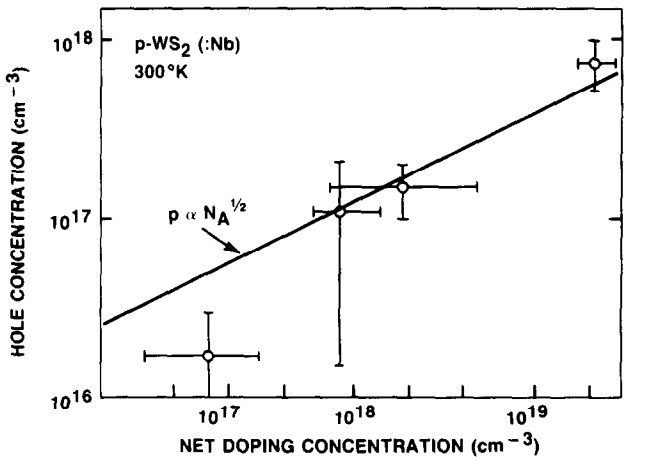

FIG. 7. Comparison of net hole versus net doping concentration indicating $p \propto N_A^{1/2}$ behavior in the region 1×10^{17} to 1×10^{18} hole concentration.

in both n- and p-WS_2 is shown in Fig. 8. The results demonstrate that at higher temperatures, the mobility increases with decreasing temperature; this result is similar to those found in other layered compounds. This behavior can be associated with phonon scattering (*22*). At lower temperatures, the mobility increases with increasing temperature, which is consistent with an ionic scattering model (*22*). Such scattering is also associated with the presence of growth steps in the crystal. Quantitative interpretation of low temperature transport data, which were strongly dependent on the sample quality, is unreliable. Qualitatively, we have found that, assuming noncompensated materials, the activation energy of donor impurities in n-WS_2 is $\simeq$0.25 eV. The activation energy of acceptors in p-WS_2 is $\simeq$0.1 eV. These results are consistent with an effective mass (m^*) of both electrons and holes as $0.5 \leq m^* \leq 1$.

Conclusions

Single crystals of n-WS_2 are grown by chemical vapor transport in 30-ml silica tubes containing 37 mg/ml of tube of WS_2, with either bromine (5.5 mg/ml of tube) or chlorine (0.3 to 3.0 mg/ml of tube) as transport agents. The most important parameter is the temperature of the growth zone, and this should be kept $\simeq$1150°C. The nature or concentration of the transporting agents and the amount of charge within the transport tube are important. Single crystals of

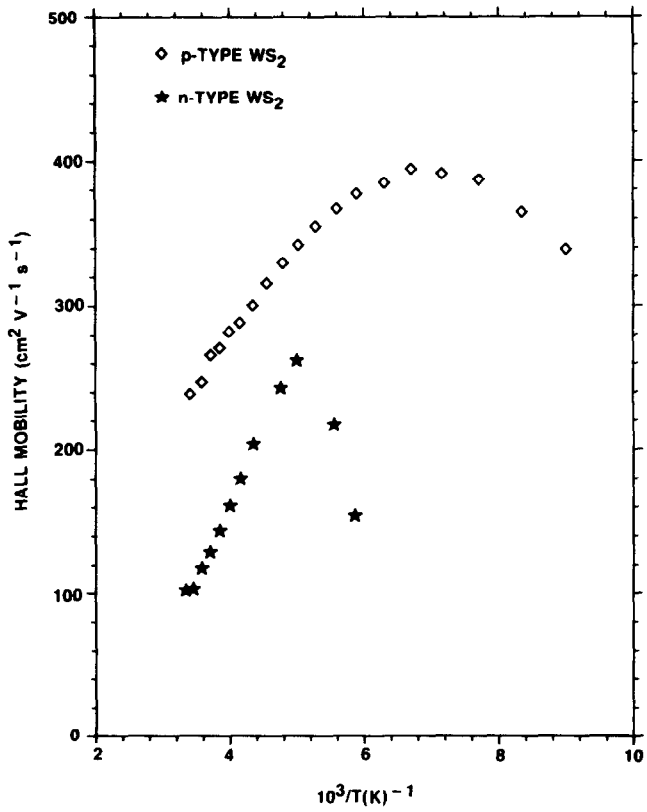

FIG. 8. Mobility versus temperature for n- and p-WS_2.

p-WS_2 can also be grown by chlorine vapor transport at the same temperature by preparing a charge containing a relatively high concentration of niobium. Using ≈37 mg$((1 - x)WS_2 \cdot xNbS_2)$/ml of tube with 3 mg Cl_2/ml of tube, the best crystals were obtained when $0.005 < x < 0.05$. Thermodynamic analysis explains the nature of the transporting species and the observation that silicon is not a significant contaminant in WS_2. Also, the thermodynamic analysis demonstrates why an appreciable concentration of niobium in the charge is necessary to form ppm doping levels in the crystals.

Transport measurements demonstrated that the doping and carrier concentrations in p-WS_2 are dependent on the niobium concentration. The heating of a charge (≈ 37 mg WS_2/ml of tube and transport agent of 3 mg Cl_2/ml of tube in a 30-ml silica tube) to temperatures ≈1200°C with $\Delta T \approx 50$ results in the formation of n-WS_2. The net doping concentration of n-WS_2 is 3×10^{16}, while the carrier concentration is $\approx 2 \times 10^{15}$. Subjecting samples formulated as $(1 - x)WS_2 \cdot xNbS_2$ to the same conditions as with n-WS_2 resulted in p-type crystals. The net doping concentrations increased from $\approx 5 \times 10^{16}$ to 1×10^{19}, while the carrier concentrations increased from 2×10^{16} to 1×10^{18} when x was increased from 0.005 to 0.05.

At doping levels above 10^{17} ($x > 0.01$) the conductivity of the crystals is dominated by acceptor levels (not compensated) which are located about 0.1 eV above the valence band. These levels are attributed to niobium substitution into tungsten sites within the structure. The donor states in n-WS_2 are located at about 0.25 eV below the conduction band. The nature of these states has not been established. It is believed that donor states are associated with sulfur deficiencies which in turn are favored at higher temperatures, viz., $WS_2 = WS_{2-x} + xS$. Attempts to correlate the change in carrier concentrations in single crystals with changes in S/W ratio within the charge were, however, unsuccessful. Finally, these compounds have been used in photoelectrochemical systems and have demonstrated encouraging conversion efficiencies with reasonable stability against corrosion (*11*).

Acknowledgments

The authors acknowledge the support of GTE Laboratories, Inc. In addition, the work done at Brown University was supported in part by GTE (J.M.) and NSF-SSC Grant DMR-82-03667 (K.D.). The use of the facilities of the NSF Materials Research Laboratory at Brown University is also acknowledged. Finally, the authors thank Mr. Robert Kershaw for performing Hall effect measurements and Mr. Greg Parsons for performing capacitance voltage measurements.

References

1. (a) H. TRIBUTSCH, *Z. Naturforsch. A* **32,** 972 (1977); (b) H. TRIBUTSCH AND J. C. BENNETT, *J. Electroanal. Chem. Interfacial Electrochem.* **81,** 97 (1977); (c) H. TRIBUTSCH, *Ber. Bunsenges. Phys. Chem.* **82,** 169 (1978); (d) H. TRIBUTSCH, *J. Electrochem. Soc.* **125,** 1086 (1978); (e) J. GOBRECHT, H. GERISCHER, AND H. TRIBUTSCH, *J. Electrochem. Soc.* **125,** 2085 (1978); (f) H. TRIBUTSCH, T. SAKATA, AND T. KAWAI, *Electrochem. Acta* **26,** 21 (1981).
2. (a) W. KAUTEK AND H. GERISCHER, *Surf. Sci.* **119,** 46 (1982); (b) W. KAUTEK, J. GOBRECHT, AND H. GERISCHER, *Ber. Bunsenges. Phys. Chem.* **84,** 645 (1980).
3. H. J. LEWERENZ, A. HELLER, AND F. J. DISALVO, *J. Am. Chem. Soc.* **102,** 1877 (1980).
4. L. C. UPADHYAYULA, J. J. LOFERSKI, A. WOLD, W. GIRIAT, AND R. KERSHAW, *J. Appl. Phys.* **39,** (10), 4736 (1968).
5. A. A. AL-HILLI AND B. L. EVANS, *J. Cryst. Growth* **15,** 93 (1972).
6. F. LEVY, P. H. SCHMID, AND H. BERGER, *Philos. Mag.* **34,** 1129 (1976).
7. H. SCHAFER, T. GROFE, AND M. TRENKEL, *J. Solid State Chem.* **8,** 14 (1973).
8. M. K. AGARWAL, H. B. PATEL, AND K. NAGI REDDY, *J. Cryst. Growth* **41,** 84 (1977); M. K. AGARWAL, K. NAGI REDDY, AND H. B. PATEL, *J. Cryst. Growth* **46,** 139 (1979).
9. J. C. WILDERVANCK, thesis, State University Gronengen (1970).
10. G. KLINE, K. K. KAM, R. ZIEGLER, AND B. A. PARKINSON, *Sol. Energy Mater.* **6,** 337 (1982).

11. (a) J. A. BAGLIO, G. S. CALABRESE, E. KAMIENIECKI, R. KERSHAW, C. P. KUBIAK, A. J. RICCO, A. WOLD, M. S. WRIGHTON, AND G. D. ZOSKI, *J. Electrochem. Soc.* **129,** 1461 (1982). (b) J. A. BAGLIO, G. S. CALABRESE, D. J. HARRISON, E. KAMIENIECKI, A. J. RICCO, M. S. WRIGHTON, AND G. D. ZOSKI, *J. Am. Chem. Soc.* **105,** 2246 (1983).

12. G. GORDON AND B. MCBRIDE, NASA Report SP-273, Washington, D.C. (1976).

13. JANAF Thermochemical Tables, 2nd ed., Dow Chemicals, Midland, Mich. (1971).

14. JANAF Thermochemical Tables, 1978 Supplement, *J. Phys. Chem. Ref. Data* **7,** 793 (1978).

15. G. DITTMER AND U. NIEMANN, *Philips J. Res.* **36,** 89 (1981).

16. H. SCHAFER AND F. SCHULTE, *Anorg. Allg. Chem.* **405,** 307 (1974).

17. P. A. O'HARE, E. BENN, F. YU CHENG, AND G. KUZNYCK, *J. Chem. Thermodyn.* **2,** 797 (1970).

18. K. C. MILLS, "Thermodynamic Data for Inorganic Sulfides, Selenides, and Tellurides," Butterworths, London (1974).

19. A. A. BALCH *in* "Crystallography and Crystal Chemistry of Materials with Layered Structures" (F. Levy, Ed.), Vol. 2, Reidel, Dordrecht-Holland/Boston (1976).

20. R. PRATAP AND R. K. GUPTA, *Phys. Status Solidi A* **9,** 415 (1972).

21. E. Kamieniecki, *J. Vac. Sci. Technol.* **20,** 811 (1982).

22. S. M. Sze, "Physics of Semiconductor Devices," Wiley, New York (1969).